
Article:
Bernut, A. orcid.org/0000-0002-1928-8329, Le Moigne, V., Lesne, T. et al. (3 more authors) (2014) In vivo assessment of drug efficacy against Mycobacterium abscessus using the embryonic zebrafish test system. Antimicrobial Agents and Chemotherapy, 58 (7). pp. 4054-4063. ISSN 0066-4804

https://doi.org/10.1128/aac.00142-14

AAC Accepts, published online ahead of print on 5 May 2014
Antimicrob. Agents Chemother. doi:10.1128/AAC.00142-14

In vivo assessment of drug efficacy against *Mycobacterium abscessus* using the embryonic zebrafish test system

Audrey Bernut[1], Vincent Le Moigne[3], Tiffany Lesne[1], Georges Lutfalla[1], Jean-Louis Herrmann[3] and Laurent Kremer[1,2,#]

[1]Laboratoire de Dynamique des Interactions Membranaires Normales et Pathologiques, CNRS UMR5235, Université Montpellier 2, Montpellier, France ;

[2]Inserm, DIMNP, Place Eugène Bataillon, 34095 Montpellier Cedex 05, France.

[3]EA3647-EPIM, UFR des Sciences de La Santé; Université de Versailles St Quentin, 2 avenue de la Source de la Bièvre, 78180 Montigny le Bretonneux, France.

[#]To whom correspondence should be addressed:

Tel: (+33) 4 67 14 33 81, Fax: (+33) 4 67 14 42 86, E-mail: laurent.kremer@univ-montp2.fr

Keywords: *M. abscessus*, zebrafish, drug testing, optical imaging, infection

Running title: *In vivo* imaging for anti-*M. abscessus* drug testing

ABSTRACT

Mycobacterium abscessus is responsible for a wide spectrum of clinical syndromes and is one of the most intrinsically drug-resistant mycobacterial species. Recent evaluation of the *in vivo* therapeutic efficacy of the few potentially active antibiotics against *M. abscessus* was essentially performed using immune-compromised mice. Herein, we assessed the feasibility and sensitivity of fluorescence imaging for monitoring the *in vivo* activity of drugs against acute *M. abscessus* infection using zebrafish embryos. A protocol was developed where clarithromycin and imipenem were directly added to water containing fluorescent *M. abscessus*-infected embryos in a 96-well plate format. The status of the infection with increasing drug concentrations was visualized on a spatiotemporal level. Drug efficacy was assessed quantitatively by measuring the index of protection, the bacterial burden (CFU) and the number of abscesses through fluorescence measurements. Both drugs were active in infected embryos and were capable of significantly increasing embryo survival in a dose-dependent manner. Protection from bacterial killing correlated with restricted mycobacterial growth in the drug-treated larvae and with reduced pathophysiological symptoms, such as the number of abscesses within the brain. In conclusion, we present here a new and efficient method for testing and compare the *in vivo* activity of two clinically-relevant drugs based on a fluorescent reporter strain in zebrafish embryos. This approach could be used for rapid determination of *in vivo* drug susceptibility profile of clinical isolates and to assess the preclinical efficacy of new compounds against *M. abscessus*.

45 **INTRODUCTION**

46

47 The emerging pathogen *M. abscessus* (*Mabs*) is the etiological agent of a wide spectrum
48 of infections in humans including severe chronic pulmonary and disseminated infections,
49 mostly in immunosuppressed and in cystic fibrosis (CF) patients (1), and cutaneous diseases,
50 often post-traumatic and post-surgical. This neglected pathogen causes a higher fatality rate
51 than other Rapidly Growing Mycobacteria (RGM) and CF patients infections is becoming a
52 major threat in most CF centers worldwide (2). *Mabs* infections occur in early childhood (3),
53 are severe and sometimes fatal, especially following transplantation (4-6), and may lead to
54 outbreaks of infection (6). It is also the main RGM responsible for nosocomial and iatrogenic
55 infections in humans (post-injection abscesses, cardiac surgery, and plastic surgery) (7-9). It
56 has been reported to cross the blood-brain barrier and cause important central nervous
57 system (CNS) lesions. Although rapid grower, *Mabs* possesses several important pathogenic
58 traits such as the ability to i) persist silently for years and even decades (10) in the human
59 host, and to ii) induce lung disease with caseous lesions and granuloma formation in the
60 parenchyma (11, 12).

61 The major issue with *Mabs* relies on its intrinsic resistance to the most available
62 antibiotics. The American Thoracic Society has recommended different groups of agents,
63 namely macrolides (clarithromycin), aminoglycosides (amikacin), cephamycins (cefoxitin)
64 and carbapenems (imipenem) to treat *Mabs* infections (13). Patients with severe infections
65 are generally treated with long courses of combinatorial antibiotic therapy, often backed by
66 surgical resection. As antibiotic susceptibility testing is not fully standardized, the clinical
67 response to drugs does not correlate well with *in vitro* susceptibility tests and failure occurs
68 frequently despite administration of two or three antibiotics for several months (14). This

69 further emphasizes the need for suitable animal models (15, 16). In addition, different
70 clinical isolates of this emerging pathogen are not uniformly susceptible to currently used
71 antibiotics (17). As a consequence, an optimal regimen to cure the *Mabs* infections has not
72 been yet established.

73 Thanks to the recent availability of efficient genetic tools (18), *Mabs* has been proposed
74 as an attractive experimental model to study non-tuberculous mycobacteria associated
75 diseases. Our poor understanding of the pathogenesis of *Mabs,* essentially hampered by the
76 restricted panel of cellular/animal models available, prompted us to develop the zebrafish
77 (ZF) model of infection evaluate *Mabs* infections (19). In particular, the *Mabs*/zebrafish
78 model already provided important insights into *Mabs* pathogenesis including the unexpected
79 CNS tropism, a finding relevant in the light of recent clinical studies reporting the presence
80 of *Mabs* in the CNS of infected human patients (20, 21). Since infection foci/abscesses within
81 the CNS, particularly the brain, appear very rapidly and are easily visualized, we reasoned
82 that this alternative model could represent a valuable and cheap system to evaluate and
83 compare the *in vitro* and *in vivo* activity of drugs against *Mabs*. Such a simple and innovative
84 system would be particularly suited to screen active molecules and/or assess antibacterial
85 activities for the discovery of the urgently needed drugs to fight *Mabs*.

86 Here, we report experimental conditions for spatiotemporal *in vivo* imaging of *Mabs*
87 infections and their use to test the efficacy of drug treatments. This represents a unique
88 biological model allowing non-invasive observations to evaluate, in real time, the efficacy of
89 antibiotics in living infected vertebrates, a system that could be applied to high-throughput
90 *in vivo* testing of drug efficacy against the most drug-resistant mycobacterial species.
91

MATERIALS AND METHODS

M. abscessus strains and growth conditions

The rough variant of *M. abscessus sensu stricto* strain CIP104536^T (ATCC19977T) (R-*Mabs*) was grown at 30°C in Middlebrook 7H9 broth supplemented with 10% Oleic acid/Albumin/Dextrose/Catalase (OADC) enrichment and 0.05% Tween 80 (7H9^T) or on Middlebrook 7H10 agar containing 10% OADC (7H10). Recombinant *Mabs* carrying pTEC27 (Addgene, plasmid 30182) that allows to express the tdTomato fluorescent protein under the control of a strong mycobacterial promoter were grown in the presence of hygromycin 500 mg/L (19).

Mice experiments and CFU counting

6-8 weeks old BALB/c mice were divided in groups of 5-7 mice and used for either intravenous (*i.v.*) or aerosol challenges. Inocula were prepared from rapidly thawed frozen aliquots, and bacterial clumps were eliminated by iterative passages through a 29.5-gauge insulin needle (Becton Dickinson). Bacterial suspensions were then diluted in phosphate buffer saline (PBS). For *i.v.* inoculations, 10^6 CFU (in 200 µl) were injected into the lateral tail/caudal vein, as previously described (22, 23). Pulmonary infections were achieved with aerosolized *Mabs* using an aerosol generator, equipped with a Micro Mist® small volume nebulizer (Hudson RCI-Teleflex medical) containing 6 ml of bacterial solution at 4×10^7 CFU/ml. Pre-sleeping mice (isoflurane® Abbott) were anesthetized with 200 µl of Hypnomidate (Etomidate®, Janssen-Cilag) and placed into an opened 50 ml syringe fixed on the top of a closed compartment containing the nebulizer. In this device, nebulization lasted for 15 min to vaporize the entire bacterial suspension. Lungs, liver and spleen were collected

in PBS, crushed and 10-fols serial dilutions were plated on Middlebrook 7H11 plates for CFU counting, as previously described (22, 23). Plates were then incubated at 37°C for up to 7 days. The results were expressed as the mean Log_{10} CFU per organ.

Minimal inhibitory concentrations

Antibiotics powder tested in drug susceptibility assays were pharmaceutical standards for imipenem/cilastatin (Mylan) or clarithromycin (Sigma-Aldrich). Stock solutions were dissolved in water (imipenem) or in DMSO (clarithromycin). Drug susceptibility testing was also determined using the microdilution method, in cation-adjusted Mueller-Hinton broth, according to the Clinical and Laboratory Standards Institute (CLSI) guidelines (24). In addition, the susceptibility profile was also determined on LB agar supplemented with increasing concentrations of compounds. Serial 10-fold dilutions of each actively growing culture were plated and incubated at 37°C for 3-4 days and the MIC was defined as the minimum concentration required to inhibiting 99% of the growth.

Zebrafish care and ethic statements

All zebrafish experiments were done at the University Montpellier 2, according to European Union guidelines for handling of laboratory animals (http://ec.europa.eu/environment/chemicals/lab_animals/home_en.htm) and approved by the Direction Sanitaire et Vétérinaire de l'Hérault and Comité d'Ethique pour l'Expérimentation Animale de la région Languedoc Roussillon (CEEA-LR) under the reference CEEA-LR-13007. Experiments were done using the *golden* ZF mutant (25), maintained as described earlier (19). Ages of embryos are expressed as hours post fertilization (hpf).

Microinjection of *M. abscessus* into embryos

Mid-log phase cultures of *Mabs* expressing tdTomato were centrifuged, washed and resuspended in PBS supplemented with 0.05% Tween-80 (PBS^T). Bacterial suspensions were then homogenized through a 26-gauge needle and sonicated and the remaining clumps were allowed to settle down to for 5-10 min, as previously described (19). Bacteria were concentrated to an OD_{600} of 1 in PBS^T and *i.v.* injected (≈2nL containing 300 CFU) into the caudal vein in 30hpf embryos previously dechorionated and anesthetized. To follow infection kinetics and embryo survival, infected larvae were transferred into 96 well plates (2 embryos/plate) and incubated at 28.5°C. The inoculum size was checked by injection of 2nL in sterile PBS^T and plated on 7H10 supplemented with hygromycin 500 mg/L.

Drug efficacy assessment in *Mabs*-infected ZF

Clarythromycin and imipenem/cilastatin were added at one day post-infection (dpi), directly into the water containing the embryos. Three doses were tested, corresponding to 1.7X, 17X and 170X the MIC of clarithromycin and 0.5X, 5X or 28X the MIC of imipenem, based on the values determined using the microdilution method (Table S1). *In vivo* drug efficacy was determined for each concentration by following i) bacterial burdens, ii) kinetics of embryo survival, iii) evolution of the infection foci/abscesses within the CNS and iv) effect on bacterial cord formation/reduction. Survival curves were determined by recording dead embryos (no heartbeat) every day for up to 13 days. Regarding the kinetic of mycobacterial loads, groups of three infected embryos were collected, lysed individually in 2% Triton X100-PBS^T with a 26-gauge needle and resuspended in PBS^T. Several 10-fold dilutions of homogenates were plated on 7H10, the appropriate antibiotics and added of mix of "BBL^{TM}

MGIT™ PANTA™“ (Becton-Dickinson) using as recommended by the supplier. CFU were enumerated after 4 days of incubation at 30°C. This procedure was repeated at 0, 3, 5 dpi.

Microscopy

Widefield bright-field and fluorescence live microscopy of infected embryos were performed using an Olympus MVX10 epifluorescent microscope equipped with a X-Cite®120Q (Lumen Dynamics) 120W mercury light source. Images are acquired with a digital color camera (Olympus XC50) and processed using CellSens software (Olympus). Fluorescence filter cube TRITC-MVX10 is used for detection of red light. For live imaging, anesthetized infected embryos were positioned in dishes and immobilized with 1% low-melting point agarose solution covering the entire larvae then immobilized embryos are immersed with fish water containing tricaine for direct visualization.

Image Processing and Analysis

Final images analysis and visualization are performed using GIMP 2.6 freeware to merge fluorescent and DIC images and to adjust levels and brightness and to remove out-of-focus background fluorescence.

Statistical Analyses

Statistical analyses of comparisons between Kaplan-Meier survival curves were performed using the log rank test with Prism 4.0 (Graphpad, Inc). CFU counts and quantifications experiments were analyzed using one-way ANOVA and Fisher's exact test, respectively. Statistical significance was assumed at p values <0.05.

187 **RESULTS**

188 ***M. abscessus* fails to establish a persistent infection in BALB/c mice**

189 Experiments were first aimed at determining the colonization rate of R-*Mabs* in a murine
190 pulmonary infection model (Figure 1A). Aerosol infections of BALB/c mice led to an initial and
191 rapid increase of the bacterial burden from 1-3 days post-infection (dpi) in the lungs, followed
192 by a phase of infection control leading to a reduction (starting after 3dpi) and almost
193 complete clearance of the bacilli at 27dpi. Very few bacteria were detected within the spleen
194 or the liver of infected mice. The colonization profile after *i.v.* challenge showed that bacilli
195 were primarily found in the liver at 1dpi and to a lesser extent in the spleen and lungs (Figure
196 1B). All heavily infected organs rapidly underwent a progressive reduction in bacterial loads
197 with a 3-Log_{10} CFU decrease in the liver and lungs at 30dpi, highlighting a transient
198 colonization process. This indicates that immune-competent mice steadily eradicate the
199 pathogen and therefore that wild-type BALB/c mice are not well adapted to investigate the *in*
200 *vivo* efficacy of therapeutic treatments. This would require testing a very large number of
201 animals to insure that the observed CFU decrease results from an antibiotic regimen rather
202 than from the natural course of infection. This highlights the need of an alternative animal
203 model, susceptible to *Mabs* infection, permissive to bacterial replication and leading to the
204 development of infection foci/abscesses and death. Therefore, the ZF embryo model was
205 chosen to test *in vivo* assessments of drugs against *Mabs*.

206

207 **Zebrafish larvae for *in vivo* assessment of drug activity in *M. abscessus***

208 An experimental protocol was designed to assess *in vivo* antimycobacterial drug activity
209 against *Mabs* in ZF larvae (Figure 2). Red fluorescent tdTomato-expressing R-*Mabs* were
210 injected in the caudal vein of embryos at 30 hours post-fertilization (hpf) and transferred

211 into 96-well plates. Antibiotics were directly added at 1dpi to the water containing the
212 infected embryos and the drug-supplemented water was then changed on a daily basis for 5
213 days. Thanks to the optical transparency of the embryos, daily microscopic recording of
214 mortality (transmission) as well as bacterial burden (fluorescence) were used as phenotypic
215 read-outs. We have previously shown that the rough *Mabs* exhibits a marked neurotropism
216 with massive abscesses within the CNS (19), thus prompting us to assess the
217 chemotherapeutic activity of drugs in *Mabs*-infected embryos with a special emphasis on
218 infection within the CNS (Figure 2). Drug-mediated toxicity was investigated by checking
219 survival curves of non-infected embryos treated with increasing drug doses.
220
221 **Minimal inhibitory concentrations of antimycobacterial drugs against *M. abscessus***
222 We first determined the *in vitro* activity of various drugs, including antitubercular
223 agents, against *Mabs* using microdilution in cation-adjusted Mueller-Hinton broth, according
224 to the Clinical and Laboratory Standards Institute guidelines (24). Table S1 shows that the
225 activity varies considerably, in agreement with other studies (17). The first-line
226 antitubercular drug isoniazid and second-line drug thiacetazone appeared inactive against
227 *Mabs*. Among the few clinically used drugs for the treatment of *Mabs* infection, cefoxitin,
228 amikacin, imipenem and erythromycin exhibit moderate activity *in vitro* on agar plates with
229 MICs ranging from 60-125 µM, whereas clarithromycin demonstrated the highest activity
230 with an MIC value of 4 µM. Because clarithromycin and imipenem exhibit different
231 physicochemical properties (high molecular weight and hydrophobicity for clarithromycin
232 versus low molecular weight and hydrophilicity for imipenem), they were further
233 investigated for their *in vivo* therapeutic efficacy in *Mabs*-infected ZF.
234

235 ***In vivo* susceptibility of *M. abscessus* to clarithromycin**

236 Due to poor information concerning the mechanisms of drug uptake by ZF
237 embryos/larvae, we tested a wide range of clarithromycin concentrations: 6.6 µM to 668 µM
238 (1.7X to 170X the *in vitro* MIC value from the microdilution method). Supplementing the
239 embryo-containing water with low or intermediate doses (1.7X and 17X the MIC,
240 respectively) led to no toxicity as measured by larval survival, while the highest tested dose
241 (170X MIC), led to a 10% reduction in larval survival at 9dpi, with respect to the control
242 group (water with 1% DMSO; Figure 3A) (26). In the presence of high doses of
243 clarithromycin, embryos had a curved body trunk with un-inflated swim bladder (Figure 3A,
244 inset). These phenotypic alterations were hardly observed when exposed to intermediate or
245 low doses of clarithromycin (not shown).

246 No significant increased survival was found when infected-embryos were exposed to
247 low and intermediate drug concentrations (Figure 3B). In contrast, high doses extended the
248 life span of infected embryos and fully protected the infected embryos up to 9dpi, when the
249 first embryo started to dye, which coincidently, corresponded to the toxicity-induced-killing
250 effect (Figure 3A). This shows that clarithromycin, using the highest regimen, is efficient in
251 the ZF test system.

252

253 **Effects of clarithromycin on ZF survival, bacterial burden and abscesses**

254 Increased survival was associated with lower bacterial burdens after 3dpi in the
255 presence of the highest dose (170X MIC), as determined quantitatively by CFU plating
256 (Figure 3C), whereas treatment with the low or intermediate doses failed to restrict
257 mycobacterial growth. *In vivo* drug efficacy was next monitored by time-lapse fluorescence
258 microscopy (Figure 3D) of the rapidly growing infection foci and abscesses in the larval brain

(19). Imaging the same infected embryos at 3 and 5dpi revealed that abscesses within the brain were already reduced at 3dpi when treated with high drug concentrations and this reduction of the clinical signs of infection was even more accentuated at 5dpi. Consistent with the survival curves and kinetic of bacterial growth, there was no visible reduction of the infection at 5dpi in ZF treated with low or intermediate drug concentrations. Quantitative analysis reveals that high doses of clarithromycin reduced by 50% the number of embryos with abscesses (Figure 3E) both in the brain and the spinal cord (Figure 3F). This indicates that clarithromycin exerts a therapeutic effect by inhibiting mycobacterial growth, preventing the development of abscesses within the CNS and protecting the embryos from bacterial killing.

Effects of imipenem on ZF survival and reduction of the pathological signs

Imipenem is a clinically relevant drug against *Mabs* known to act on L, D-transpeptidases (17, 27). Concentrations from 0.5X to 28X MIC of imipenem were tested, which all fail to display signs of toxicity-induced-killing or developmental abnormalities (data not shown). When assessing the effect of imipenem on infected ZF, no increased survival was found with low drug concentrations. However, treatment with intermediate doses led to a significant increase in survival and 100% of protection was observed in the presence of the highest drug concentration (Figure 4A). These survival rates correlated with CFU loads as intermediate and high doses of imipenem started to restrict bacterial growth at 3dpi (after two days of drug treatment) (Figure 4B). With the highest dose, there was a 3 Log_{10} decrease in CFU at 5dpi (four days of treatment) compared with the untreated control group. Time-lapse fluorescence microscopy further confirmed the *in vivo* efficacy of imipenem at intermediate and high doses, illustrating the inhibition of bacterial growth and disappearance of abscesses

in the larval brain at 3 and 5dpi, respectively (Figure 4C). High doses significantly reduced the proportion of embryos with abscesses (Figure 4D), a phenotypic effect that was particularly apparent in the brain on infected embryos (Figure 4E), indicating that imipenem reduces the pathology signs of the infection.

These results prompted us to check whether imipenem can counteract/alter the progression of an already established infection, if given at 3dpi when brain abscesses are already apparent (Figure S1A). Death curves indicate that treatment with high doses of imipenem efficiently extended the life span of embryos with pre-existing abscesses (Figure S1B). A large proportion (more than 60%) of the treated embryos survived to the infection compared to 10% for the non-treated individuals (p=0.008). The 40% embryos that died despite treatment showed increased bacterial loads in the CNS (data not shown). The increased index of protection rate was associated to a significant decrease in the number of embryos with abscesses (Figure S1C), particularly within the brain (Figure S1D). This "curative" protocol shows that imipenem was able to cure embryos with pre-existing abscesses and protect severely infected ZF.

***In vivo* inhibition activity of imipenem on mycobacterial cording**

Rough *Mabs* displays a dry texture with organized serpentine cords on agar plates (19, 28, 29) and large bacterial clumps consisting mainly of cords in liquid cultures (19). Our recent studies also unraveled the presence of serpentine cords within the brain or spinal cord of embryos infected with the rough morphotype and emphasized the role of cording in immune evasion by preventing phagocytosis of *Mabs* by macrophages and neutrophils (19). Cords are easily visualized and counted by fluorescence microscopy (Figure 5A), and they promote extracellular replication, abscess formation and tissue damage (19). We checked

whether exposure of infected embryos to imipenem may affect the development of mycobacterial cords. Figure 5B shows the impact of imipenem treatment on the number of cords; quantitative analysis is shown in Figure 5C. The presence of low doses of imipenem has little impact on mycobacterial cords, although a reduction of the number of embryos with cords was detected at 4dpi. However, this effect was more pronounced with higher drug concentrations with only 20% of cord-laden embryos at 4dpi (compared to 60% for untreated embryos at 4dpi). This dose-dependent effect occurred essentially within the CNS whilst reduction of cord formation within the vasculature was not significant (Figure 5D).

316 **DISCUSSION**

317 At a basic research level, the appropriate use of animal models can help to improve our
318 understanding of host-pathogen interactions. At a more applied level, preclinical evaluation
319 of new drugs requires *in vivo* testing prior to progressing along the development pipeline.
320 However, *in vivo* animal studies, when possible, are usually costly and time-consuming and
321 present a major bottleneck in drug developments. Implementation of novel approaches,
322 expected to accelerate the *in vivo* assessment of drugs, is particularly justified in two cases.
323 First, such systems are useful for bacterial infections requiring extended periods of drug
324 treatment such as mice infected with *M. tuberculosis,* for which rapid *in vivo* assessment of
325 drug efficacy directly in infected mice using fluorescence imaging (30) or using improved
326 firefly luciferase (31) were elegantly demonstrated. We similarly show in this study how the
327 use of fluorescence imaging can be useful in evaluating antimicrobial activity against *Mabs*.
328 Second, alternative biological systems are particularly relevant for infections lacking of a
329 permissive animal model. In this context, we recently demonstrated the high susceptibility of
330 ZF embryos to *Mabs* (19) and how the number of CNS abscesses may represent a marker for
331 establishing *in vivo* antibiotic activity against *Mabs*.

332 One of the key steps of drug discovery process is to identify and evaluate the *in vitro* and
333 *in vivo* potential of new hits against *Mabs* using adapted animal models. The murine model
334 in immune-competent BALB/c mice (*i.v.* or aerosol infections), led only to transient
335 colonization, impeding its use as a valuable animal model for drug testing. Comparatively,
336 SCID mouse model has been shown to produce a chronic infection of *Mabs*, but this model
337 has not been used for drug testing (29, 32). Granulocyte-macrophage colony-stimulating
338 (GM-CSF) knockout mice have recently been used to develop a new animal model of
339 persistent pulmonary *Mabs* infection that can be used for preclinical efficacy testing of anti-

340 microbial drugs (15). Azithromycin treatment of *Mabs*-infected GM-CSF KO mice resulted in
341 a lower bacterial burden in the lungs and spleen, weight gain and significant improvement in
342 lung pathology (15). Another report proposed Nude mice as an adequate model for *in vivo*
343 chemotherapy studies (16). However, both models raised the question of the adaptive
344 response in addition to the antibiotic activity in eradicating the bacilli. It was previously
345 shown that, albeit being a rapid-growing mycobacterium, *Mabs* infection was only controlled
346 in mice with a functional adaptive immune response (22), as compared to *M. chelonae*,
347 which was cleared even in T cell-deficient mice. Despite the fact that both immune-
348 compromised mice present a significant advance as compared to wild-type mice in
349 preclinical assessments, these models remain costly, time-consuming and, most likely, not
350 suitable for a general use in drug screening strategies.

351 New non-mammalian models of infection have been developed, including *Drosophila*
352 *melanogaster* (33, 34), *Caenorhabditis elegans* (35) or *Danio rerio* (36, 37) offering
353 advantages in terms of speed, cost, technical convenience and ethical acceptability over the
354 mouse model. Except for the recent Drosophila model (34), these models have not been
355 reported for antibiotic assessments against *Mabs*. We propose here the ZF model to
356 visualize, by non-invasive imaging, the progressive infection of *Mabs* in live animals, and to
357 quantifying the effect of drug treatment. We successfully investigated the suitability and
358 sensitivity of two clinically relevant drugs, clarithromycin and imipenem, to visualize in a
359 dose- and time-dependent manner the dynamics of cord and abscess formation/resorption.
360 One major advantage of this model, compared to mice, is the ease and rapidity of
361 experimentation within a restricted time scale and low cost. That both drugs had a positive
362 impact in terms of embryo survival was correlated to a significant reduction in the number of
363 CFU and abscesses, demonstrating a proof of concept that ZF embryos are suitable for drug

efficacy testing. Since *in vitro* studies demonstrated decreased MICs in the presence of imipenem, for clarithromycin, minocycline, levofloxacin and moxifloxacin (38), future work should also address the *in vivo* efficacy of these drug combinations using the *Mabs*/ZF couple.

It is, however, noteworthy that despite their unique features for *in vivo* drug testing, ZF embryos also present several disadvantages over mammalian models. In particular, there are some important anatomical differences between ZF embryos and mammals such as gills instead of lungs, hematopoiesis occurring in the anterior kidney instead of the bone marrow, lack of discernable lymph nodes as well as a very different reproductive system. The natural lack of adaptive immunity early in the development is very likely to affect the outcome of the infection, thus making it difficult to directly correlating data obtained in ZF and in humans. In addition, as shown in this study, embryos are adapted to testing antibiotics during acute R-*Mabs* infections but not during the chronic stages of the disease, which can be better modelled for instance using immuno-compromized mice (15). Since pharmacokinetics are not known in ZF, it remains difficult at this stage to directly transpose the MIC data obtained in ZF to humans. As a consequence, this biological system should essentially be regarded as an early model for pre-clinical drug testing and/or to select new active compounds which should then be evaluated in other models before clinical trials.

The perspectives of application of the present findings are multiple. First, this method could be implemented to address the *in vivo* drug susceptibility profiles of clinical isolates including strains from CF and non-CF patients, as *Mabs* clinical strains are not uniformly susceptible to currently used antibiotics. Due to these strain-to-strain variations (17, 39), no optimal regimen has been established to cure *Mabs* infections and determining the susceptibility/resistance profile of clinical strains may greatly help the clinician to select

optimal drug treatments. It is worth mentioning that for this particular application, no absolute requirement for the tested strains to carry pTEC27 is needed, as visualization of fluorescent bacteria is not necessary if only assessing ZF survival. Second, since the ZF is particularly amenable to mimic a CF-like micro-environment, by silencing the *cftr* expression level (40), this system could be used to compare the therapeutic efficacy of clarithromycin and imipenem (and perhaps other antibiotics) in a *cftr*-deficient environment as it remains to be established whether a defect in CFTR affects susceptibility to drugs. Third, this method could be further exploited to compare the intrinsic activity of antibiotics *in vivo* in embryos infected with the three species of the *M. abscessus* complex - *M. abscessus sensu stricto*, *M. massiliense*, and *M. bolletii* - which are known to respond differently to antibiotics *in vitro* (41, 42).

Finally, the ZF embryo is particularly suited for high throughput screening as shown recently for *M. marinum* (36, 43, 44). Work is currently in progress in our laboratory to develop an *in vivo* platform for high-throughput screening of molecules against *Mabs* in order to speed up the process of identifying promising drug candidates, particularly warranted due to the extreme resistance of *Mabs* to most current antibiotics.

405 **ACKNOWLEDGMENTS**

406

407 We thank L. Ramakrishnan for the generous gift of pTEC27 and for helpful discussions. This
408 study was supported by the french National Research Agency (http://www.agence-
409 nationale-recherche.fr/) (ZebraFlam ANR-10-MIDI-009and DIMYVIR ANR-13-BSV3-0007-01),
410 the European Community's Seventh Framework Programme (FP7-PEOPLE-2011-ITN) under
411 grant agreement no. PITN-GA-2011-289209 for the Marie-Curie Initial Training Network
412 FishForPharma. We wish also to thank Vaincre La Mucoviscidose
413 (http://www.vaincrelamuco.org/) for funding A Bernut (RF2011 06000446) and V Le Moigne
414 (RF20120600689) and the InfectioPôle Sud for funding part of the fish facility.

415

416

REFERENCES

1. **Medjahed H, Gaillard JL, Reyrat JM.** 2010. *Mycobacterium abscessus*: a new player in the mycobacterial field. Trends Microbiol. **18:**117-123.
2. **Petrini B.** 2006. *Mycobacterium abscessus*: an emerging rapid-growing potential pathogen. Apmis **114:**319-28.
3. **Roux AL, Catherinot E, Ripoll F, Soismier N, Macheras E, Ravilly S, Bellis G, Vibet MA, Le Roux E, Lemonnier L, Gutierrez C, Vincent V, Fauroux B, Rottman M, Guillemot D, Gaillard JL.** 2009. Multicenter study of prevalence of nontuberculous mycobacteria in patients with cystic fibrosis in France. J. Clin. Microbiol. **47:**4124-4128.
4. **Sanguinetti M, Ardito F, Fiscarelli E, La Sorda M, D'Argenio P, Ricciotti G, Fadda G.** 2001. Fatal pulmonary infection due to multidrug-resistant *Mycobacterium abscessus* in a patient with cystic fibrosis. J. Clin. Microbiol. **39:**816-819.
5. **Gilljam M, Schersten H, Silverborn M, Jonsson B, Ericsson Hollsing A.** 2010. Lung transplantation in patients with cystic fibrosis and *Mycobacterium abscessus* infection. J. Cyst. Fibros. **9:**272-276.
6. **Aitken ML, Limaye A, Pottinger P, Whimbey E, Goss CH, Tonelli MR, Cangelosi GA, Dirac MA, Olivier KN, Brown-Elliott BA, McNulty S, Wallace RJ, Jr.** 2012. Respiratory outbreak of *Mycobacterium abscessus* subspecies *massiliense* in a lung transplant and cystic fibrosis center. Am. J. Respir. Crit. Care Med. **185:**231-232.
7. **Wallace RJ, Jr, Brown BA, Griffith DE.** 1998. Nosocomial outbreaks/pseudo-outbreaks caused by nontuberculous mycobacteria. Annu. Rev. Microbiol. **52:**453-490.
8. **Viana-Niero C, Lima KV, Lopes ML, Rabello MC, Marsola LR, Brilhante VC, Durham AM, Leao SC.** 2008. Molecular characterization of *Mycobacterium massiliense* and *Mycobacterium bolletii* in isolates collected from outbreaks of infections after laparoscopic surgeries and cosmetic procedures. J. Clin. Microbiol. **46:**850-855.

9. **Zelazny AM, Root JM, Shea YR, Colombo RE, Shamputa IC, Stock F, Conlan S, McNulty S, Brown-Elliott BA, Wallace RJ, Jr, Olivier KN, Holland SM, Sampaio EP.** 2009. Cohort study of molecular identification and typing of *Mycobacterium abscessus*, *Mycobacterium massiliense*, and *Mycobacterium bolletii*. J. Clin. Microbiol. **47:**1985-1995.

10. **Cullen AR, Cannon CL, Mark EJ, Colin AA.** 2000. *Mycobacterium abscessus* infection in cystic fibrosis. Colonization or infection? Am. J. Respir. Crit. Care Med. **161:**641-645.

11. **Tomashefski JF, Jr., Stern RC, Demko CA, Doershuk CF.** 1996. Nontuberculous mycobacteria in cystic fibrosis. An autopsy study. Am. J. Respir. Crit. Care Med. **154:**523-528.

12. **Rodriguez G, Ortegon M, Camargo D, Orozco LC.** 1997. Iatrogenic *Mycobacterium abscessus* infection: histopathology of 71 patients. Br. J. Dermatol. **137:**214-218.

13. **Griffith DE, Aksamit T, Brown-Elliott BA, Catanzaro A, Daley C, Gordin F, Holland SM, Horsburgh R, Huitt G, Iademarco MF, Iseman M, Olivier K, Ruoss S, von Reyn CF, Wallace RJ, Jr., Winthrop K.** 2007. An official ATS/IDSA statement: diagnosis, treatment, and prevention of nontuberculous mycobacterial diseases. Am. J. Respir. Crit. Care Med. **175:**367-416.

14. **Jeon K, Kwon OJ, Lee NY, Kim BJ, Kook YH, Lee SH, Park YK, Kim CK, Koh WJ.** 2009. Antibiotic treatment of *Mycobacterium abscessus* lung disease: a retrospective analysis of 65 patients. Am. J. Respir. Crit. Care Med. **180:**896-902.

15. **De Groote MA, Johnson L, Podell B, Brooks E, Basaraba R, Gonzalez-Juarrero M.** 2013. GM-CSF knockout mice for preclinical testing of agents with antimicrobial activity against *Mycobacterium abscessus*. J. Antimicrob. Chemother. **69:**1057-1064.

16. **Lerat I, Cambau E, Roth Dit Bettoni R, Gaillard JL, Jarlier V, Truffot C, Veziris N.** 2013. *In vivo* evaluation of antibiotic activity against *Mycobacterium abscessus*. J. Infect. Dis. **209:**905-912.

17. **Lavollay M, Dubee V, Heym B, Herrmann JL, Gaillard JL, Gutmann L, Arthur M, Mainardi JL.** 2014. *In vitro* activity of cefoxitin and imipenem against *Mycobacterium abscessus* complex. Clin. Microbiol. Infect. In Press.

18. **Cortes M, Singh AK, Reyrat JM, Gaillard JL, Nassif X, Herrmann JL.** 2011. Conditional gene expression in *Mycobacterium abscessus*. PLoS One **6:**e29306.

19. **Bernut A, Herrmann JL, Kissa K, Dubremetz JF, Gaillard JL, Lutfalla G, Kremer L.** 2014. *Mycobacterium abscessus* cording prevents phagocytosis and promotes abscess formation. Proc. Natl. Acad. Sci. USA **111:**E943-952.

20. **Talati NJ, Rouphael N, Kuppalli K, Franco-Paredes C.** 2008. Spectrum of CNS disease caused by rapidly growing mycobacteria. Lancet Infect. Dis. **8:**390-398.

21. **Lee MR, Cheng A, Lee YC, Yang CY, Lai CC, Huang YT, Ho CC, Wang HC, Yu CJ, Hsueh PR.** 2011. CNS infections caused by *Mycobacterium abscessus* complex: clinical features and antimicrobial susceptibilities of isolates. J. Antimicrob. Chemother. **67:**222-225.

22. **Rottman M, Catherinot E, Hochedez P, Emile JF, Casanova JL, Gaillard JL, Soudais C.** 2007. Importance of T cells, gamma interferon, and tumor necrosis factor in immune control of the rapid grower *Mycobacterium abscessus* in C57BL/6 mice. Infect. Immun. **75:**5898-5907.

23. **Catherinot E, Clarissou J, Etienne G, Ripoll F, Emile JF, Daffe M, Perronne C, Soudais C, Gaillard JL, Rottman M.** 2007. Hypervirulence of a rough variant of the *Mycobacterium abscessus* type strain. Infect. Immun. **75:**1055-1058.

24. **Woods GL, Brown-Elliott BA, Conville PS, Desmond EP, Hall GS, Lin G, Pfyffer GE, Ridderhof JC, Siddiqi SH, Wallace RJ, Warren NG, Witebsky FG.** 2011. Susceptibility testing of mycobacteria, nocardiae, and other aerobic actinomycetes; approved standard, Second Edition. M24-A2. Clinical and Laboratory Standards Institute, Wayne, PA.

25. **Lamason RL, Mohideen MA, Mest JR, Wong AC, Norton HL, Aros MC, Jurynec MJ, Mao X, Humphreville VR, Humbert JE, Sinha S, Moore JL, Jagadeeswaran P, Zhao W, Ning G, Makalowska I, McKeigue PM, O'Donnell D, Kittles R, Parra EJ, Mangini NJ, Grunwald DJ, Shriver MD, Canfield VA, Cheng KC.** 2005. SLC24A5, a putative cation exchanger, affects pigmentation in zebrafish and humans. Science **310:**1782-1786.

493 26. **Adams KN, Takaki K, Connolly LE, Wiedenhoft, Winglee K, Humbert O, Edelstein PH, Cosma**
494 **CL, Ramakrishnan L.** 2011. Drug tolerance in replicating mycobacteria mediated by a
495 macrophage-induced efflux mechanism. Cell **145:**39-53.
496 27. **Lavollay M, Fourgeaud M, Herrmann JL, Dubost L, Marie A, Gutmann L, Arthur M, Mainardi**
497 **JL.** 2011. The peptidoglycan of *Mycobacterium abscessus* is predominantly cross-linked by
498 L,D-transpeptidases. J. Bacteriol. **193:**778-782.
499 28. **Medjahed H, Reyrat JM.** 2009. Construction of *Mycobacterium abscessus* defined
500 glycopeptidolipid mutants: comparison of genetic tools. Appl. Environ. Microbiol. **75:**1331-
501 1338.
502 29. **Howard ST, Rhoades E, Recht J, Pang X, Alsup A, Kolter R, Lyons CR, Byrd TF.** 2006.
503 Spontaneous reversion of *Mycobacterium abscessus* from a smooth to a rough morphotype
504 is associated with reduced expression of glycopeptidolipid and reacquisition of an invasive
505 phenotype. Microbiology **152:**1581-1590.
506 30. **Zelmer A, Carroll P, Andreu N, Hagens K, Mahlo J, Redinger N, Robertson BD, Wiles S, Ward**
507 **TH, Parish T, Ripoll J, Bancroft GJ, Schaible UE.** 2012. A new *in vivo* model to test anti-
508 tuberculosis drugs using fluorescence imaging. J. Antimicrob. Chemother. **67:**1948-1960.
509 31. **Andreu N, Zelmer A, Sampson SL, Ikeh M, Bancroft GJ, Schaible UE, Wiles S, Robertson BD.**
510 2013. Rapid *in vivo* assessment of drug efficacy against *Mycobacterium tuberculosis* using an
511 improved firefly luciferase. J. Antimicrob. Chemother. **68:**2118-2127.
512 32. **Byrd TF, Lyons CR.** 1999. Preliminary characterization of a *Mycobacterium abscessus* mutant
513 in human and murine models of infection. Infect. Immun. **67:**4700-4707.
514 33. **Oh CT, Moon C, Jeong MS, Kwon SH, Jang J.** 2013. *Drosophila melanogaster* model for
515 *Mycobacterium abscessus* infection. Microbes Infect. **15:**788-795.
516 34. **Oh, C. T., C. Moon, O. K. Park, S. H. Kwon, and J. Jang.** 2014. Novel drug combination for
517 *Mycobacterium abscessus* disease therapy identified in a Drosophila infection model. J.
518 Antimicrob. Chemother. In Press.

519 35. **Squiban B, Kurz CL.** 2011. C. elegans: an all in one model for antimicrobial drug discovery.
520 Curr. Drug Targets **12:**967-977.
521 36. **Takaki K, Cosma CL, Troll MA, Ramakrishnan L.** 2012. An *in vivo* platform for rapid high-
522 throughput antitubercular drug discovery. Cell Rep. **2:**175-184.
523 37. **Takaki K, Davis JM, Winglee K, Ramakrishnan L.** 2013. Evaluation of the pathogenesis and
524 treatment of *Mycobacterium marinum* infection in zebrafish. Nat. Protoc. **8:**1114-1124.
525 38. **Miyasaka T, Kunishima H, Komatsu M, Tamai K, Mitsutake K, Kanemitsu K, Ohisa Y,**
526 **Yanagisawa H, Kaku M.** 2007. *In vitro* efficacy of imipenem in combination with six
527 antimicrobial agents against *Mycobacterium abscessus*. Int. J. Antimicrob. Agents **30:**255-
528 258.
529 39. **Shen GH, Wu BD, Hu ST, Lin CF, Wu KM, Chen JH.** 2010. High efficacy of clofazimine and its
530 synergistic effect with amikacin against rapidly growing mycobacteria. Int. J. Antimicrob.
531 Agents **35:**400-404.
532 40. **Phennicie RT, Sullivan MJ, Singer JT, Yoder JA, Kim CH.** 2010. Specific resistance to
533 *Pseudomonas aeruginosa* infection in zebrafish is mediated by the cystic fibrosis
534 transmembrane conductance regulator. Infect. Immun. **78:**4542-4550.
535 41. **Bastian S, Veziris N, Roux AL, Brossier F, Gaillard JL, Jarlier V, Cambau E.** 2011. Assessment
536 of clarithromycin susceptibility in strains belonging to the *Mycobacterium abscessus* group by
537 *erm(41)* and *rrl* sequencing. Antimicrob. Agents Chemother. **55:**775-781.
538 42. **Kim HY, Kim BJ, Kook Y, Yun YJ, Shin JH, Kim BJ, Kook YH.** 2010. *Mycobacterium massiliense*
539 is differentiated from *Mycobacterium abscessus* and *Mycobacterium bolletii* by erythromycin
540 ribosome methyltransferase gene (*erm*) and clarithromycin susceptibility patterns. Microbiol.
541 Immunol. **54:**347-353.
542 43. **Carvalho R, de Sonneville J, Stockhammer OW, Savage ND, Veneman WJ, Ottenhoff TH,**
543 **Dirks RP, Meijer AH, Spaink HP.** 2011. A high-throughput screen for tuberculosis
544 progression. PLoS One **6:**e16779.

44. **Spaink HP, Cui C, Wiweger MI, Jansen HJ, Veneman WJ, Marin-Juez R, de Sonneville J, Ordas A, Torraca V, van der Ent W, Leenders WP, Meijer AH, Snaar-Jagalska BE, Dirks RP.** 2013. Robotic injection of zebrafish embryos for high-throughput screening in disease models. Methods **62:**246-254.

551 **FIGURE LEGENDS**

552

553 **Figure 1. Kinetics of colonization of *M. abscessus* in aerosolised or intravenously infected**
554 **BALB/c mice. (A)** Mice were aerosolized by 4 × 10^7 CFU/ml of R-*Mabs*. Animal were then
555 sacrificed at days 1, 3, 8, 27 prior to CFU counting in the liver, spleen and lungs. Results are
556 expressed as the log units of CFU. **(B)** Mice were challenged *i.v.* 10^6 CFU of R-*Mabs.* Animals
557 were then sacrificed at days 1, 15 and 30 to determine the CFU counts in the different
558 organs. Results are expressed as mean Log_{10} CFU from 2-3 independent experiments (n=5-7
559 mice for each time point). Error bars represent the standard error of the mean (SEM).

560

561 **Figure 2. Experimental protocol to assess the *in vivo* drug activity on *M. abscessus***
562 **infection.** ZF embryos were *i.v.* infected with ≈300 CFU of R-*Mabs* expressing tdTomato and
563 distributed and incubated into 96-wells plate (1). From 1dpi, embryos were exposed to the
564 drugs of interest which were directly added to the wells. Drugs are then removed and daily
565 renewed for 5 days (2). To determinate the *in vivo* antibacterial effects of the drugs, the
566 embryo survival, the bacterial loads and the evolution of the infection process were
567 monitored at a spatiotemporal level by videomicroscopy (3).

568

569 **Figure 3. *In vivo* characterization of clarithromycin activity on *M. abscessus* infection. (A-F)**
570 Embryos were soaked in clarithromycin at 1.7X, 17X or 170X the MIC for 5 days. The red bar
571 indicates the start and duration of treatment. **(A)** Survival of uninfected embryos treated
572 with various doses of clarithromycin and compared to mock controls (DMSO 1%) (n=20 for
573 each, representative of three independent experiments). Representative microscopy image
574 of an untreated (inset, upper panel) or drug treated-embryo (inset, lower panel) at 8dpf.

575 Clarithromycin appears toxic at the highest concentration as evidenced by the development
576 of abnormalities and the increased mortality rate in the drug-exposed embryos compared to
577 the mock control (p=0.028, log-rank test). **(B)** Survival of infected *Mabs* treated at various
578 doses of clarithromycin and compared to untreated infected embryos (≈300 CFU, n=20,
579 representative of three independent experiments). A significant increased survival was
580 observed in the infected-embryos exposed to the highest drug concentration (p=0.029, log-
581 rank test). **(C)** Bacterial loads of untreated or treated-embryos (≈400 CFU). Results are
582 expressed as mean Log_{10} CFU per embryo from three independent experiments. A significant
583 reduction in bacterial burdens with 170X the MIC in drug treated-embryos is observed at
584 5dpi. **(D)** Spatiotemporal visualization of the infection by *Mabs* expressing dtTomato (≈300
585 CFU) in untreated or drug treated-embryos. The representative fluorescence and
586 transmission overlay of whole embryos are shown. The yolk is auto-fluorescent. **(E)**
587 Frequency of abscesses in whole untreated or drug treated-embryos over 13dpi (≈300 CFU;
588 average of three independent experiments). Infected embryos developed significantly less
589 abscesses in the presence of clarithromycin at 170X the MIC than untreated infected-
590 embryos. **(F)** Average localization of abscesses of the infected embryos in (E). *Mabs*-infected
591 ZF developed significantly less abscesses within the brain and the spinal when exposed to
592 the highest clarithromycin dose as compared to untreated infected-ZF. For (C) statistics were
593 calculated using one-way ANOVA or for (E) and (F) with Fisher's exact test comparing each
594 category of drug-treated embryos to untreated control. Error bars represent the SEM.
595 **p<0.01.
596
597 **Figure 4. Imipenem treatment cures *M. abscessus*-infected embryos. (A-E)** From 1dpi,
598 embryos were exposed for 5 days to imipenem concentrations corresponding to 0.5X, 5X or

28X the MIC. **(A)** Survival of infected R-*Mabs* embryos treated at various doses of imipenem and compared to untreated infected embryos (≈300 CFU, n=20, representative of three independent experiments). Survival of treated R-*Mabs* infected embryos is dose-dependent. Significant increased survival was observed in infected-embryos exposed to 5 X and 28X MIC of imipenem. The red bar indicates the start and duration of treatment. **(B)** Bacterial loads of untreated or imipenem treated-embryos (≈400 CFU). Results are expressed as mean Log_{10} CFU per embryo from three independent experiments. A significant decreased of bacterial load is already observed after 3dpi in the 28X MIC imipenem treated-embryos. **(C)** Spatiotemporal visualization of the infection by R-*Mabs* expressing tdTomato (≈300 CFU) in untreated or imipenem treated-embryos. The representative fluorescence and transmission overlay of whole embryos are shown. **(D)** Frequency of abscesses in whole untreated or imipenem-treated embryos over 13dpi (≈300 CFU, average of three independent experiments). Only the 28X MIC imipenem treated-embryos developed significantly fewer abscesses than untreated infected-embryos. **(E)** Average localization of abscesses of the infected embryos in (D). 5X and 28X MIC of imipenem treated-embryos infected by *Mabs* developed fewer abscesses within the brain than untreated infected-embryos. For (B) statistics were calculated using one-way ANOVA or for (D) and (E) with Fisher's exact test comparing each category of imipenem-treated embryos to untreated control. Error bars represent the SEM. *p=0.02, **p<0.01, ***p<0.001.

Figure 5. Imipenem treatment decreases the early pathophysiological signs within the CNS. (A-D). tdTomato-expressing R-*Mabs* (≈300 CFU) are injected in 30hpf embryos (n=15, average of three independent experiments). From 1dpi, embryos were exposed to imipenem at 0.5X, 5X or 28X MIC during 5 days. **(A)** Fluorescence microscopy of a typical R serpentine

cord. Scale bar, 100µm. **(B)** Fluorescence and DIC overlay of whole heads of a 28X MIC imipenem-treated and untreated infected embryos with fluorescent R-*Mabs* showing serpentine cord (white arrow). Scale bars, 100µm. **(C)** Percentage of embryos with cords in whole untreated and imipenem-treated embryos at 4dpi. A significant reduction in the proportion of embryos with cords was observed when embryos were treated with the highest (28X MIC) imipenem concentration. **(D)** Average localization of cord within the infected embryos in (C). Infected embryos treated with the intermediate (5X MIC) and high (28X MIC) imipenem doses developed significantly fewer serpentine cords within the CNS compared to untreated infected-embryos. For (C) and (D), statistics were calculated using Fisher's exact test comparing each category of imipenem-treated embryos to untreated control. All results are expressed as the average from three independent experiments and error bars represent the SEM.

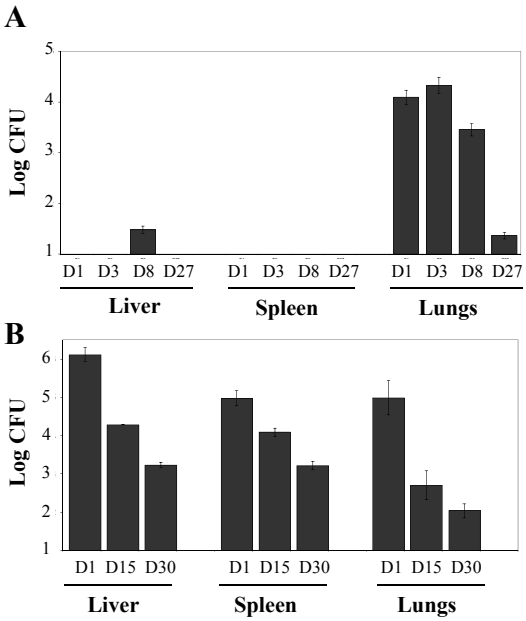

Figure 1. Kinetics of colonization of *M. abscessus* in aerosolised or intravenously infected BALB/c mice. (A) Mice were aerosolized by 4 × 10^7 CFU/ml of R-*Mabs*. Animal were then sacrificed at days 1, 3, 8, 27 prior to CFU counting in the liver, spleen and lungs. Results are expressed as the log units of CFU. **(B)** Mice were challenged *i.v.* 10^6 CFU of R-*Mabs.* Animals were then sacrificed at days 1, 15 and 30 to determine the CFU counts in the different organs. Results are expressed as mean Log_{10} CFU from 2-3 independent experiments (n=5-7 mice for each time point). Error bars represent the standard error of the mean (SEM).

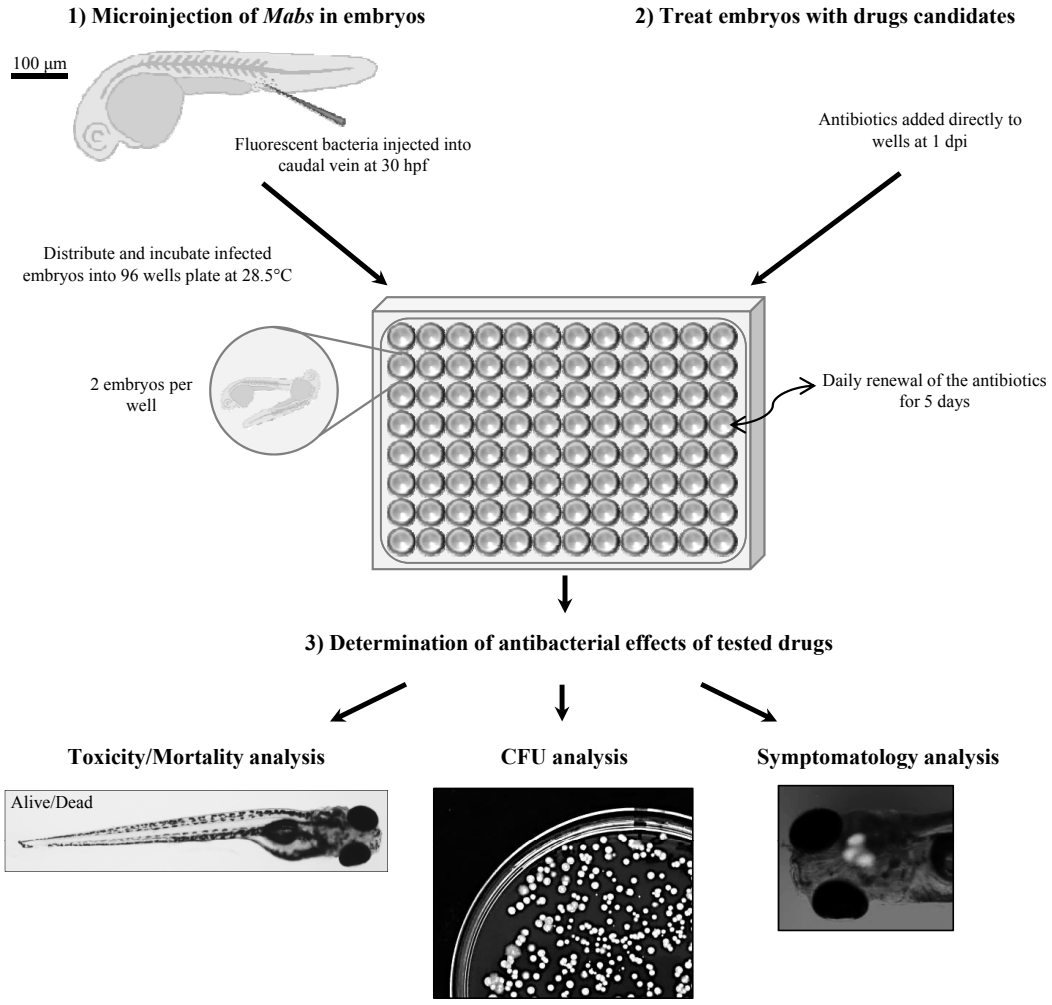

Figure 2. Experimental protocol to assess the *in vivo* drug activity on *M. abscessus* infection. ZF embryos were *i.v.* infected with ≈300 CFU of R-*Mabs* expressing tdTomato and distributed and incubated into 96-wells plate (1). From 1dpi, embryos were exposed to the drugs of interest which were directly added to the wells. Drugs are then removed and daily renewed for 5 days (2). To determinate the *in vivo* antibacterial effects of the drugs, the embryo survival, the bacterial loads and the evolution of the infection process were monitored at a spatiotemporal level by videomicroscopy (3).

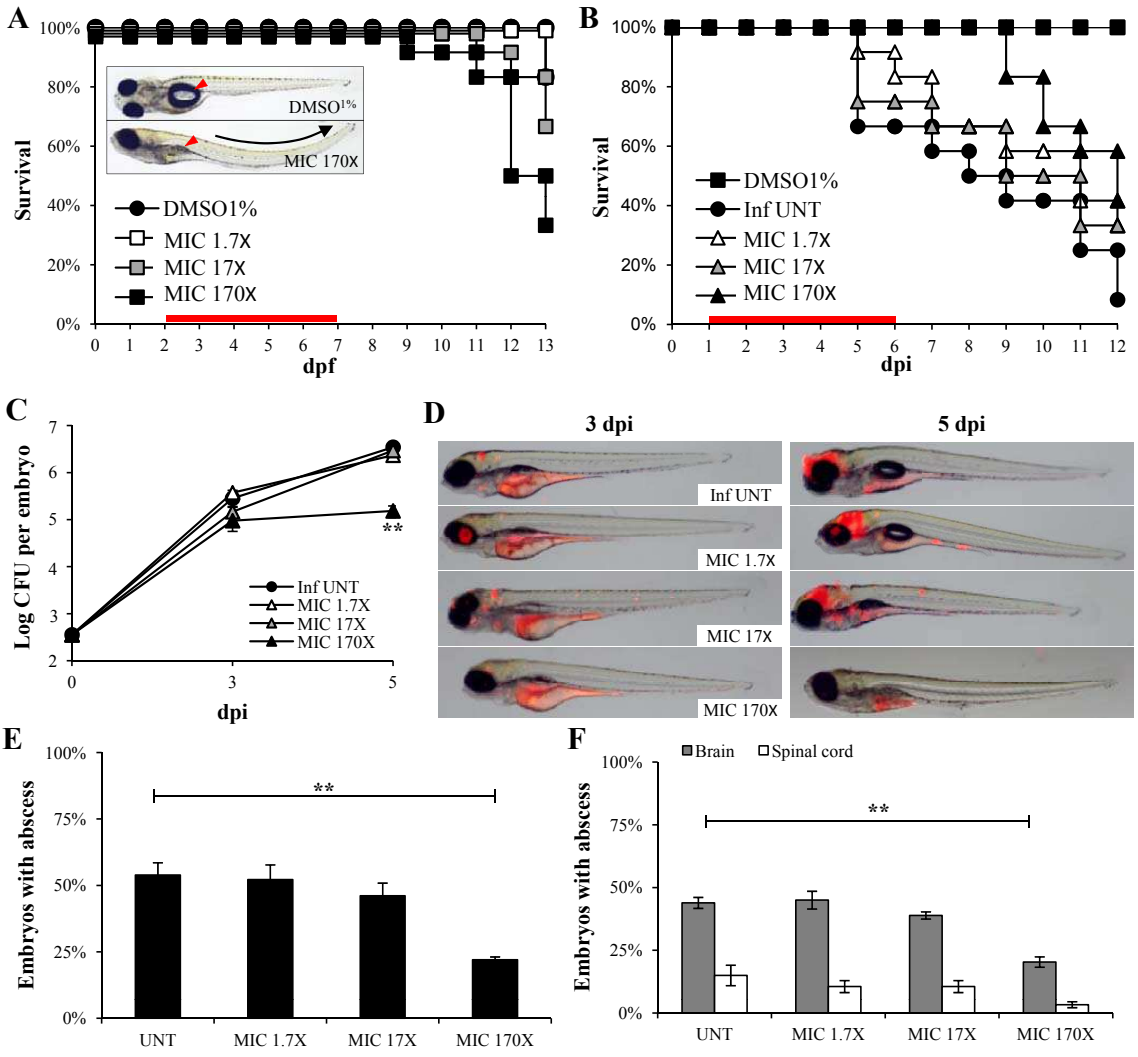

Figure 3. ***In vivo*** **characterization of clarithromycin activity on** ***M. abscessus*** **infection. (A-F)** Embryos were soaked in clarithromycin at 1.7X, 17X or 170X the MIC for 5 days. The red bar indicates the start and duration of treatment. **(A)** Survival of uninfected embryos treated with various doses of clarithromycin and compared to mock controls (DMSO 1%) (n=20 for each, representative of three independent experiments). Representative microscopy image of an untreated (inset, upper panel) or drug treated-embryo (inset, lower panel) at 8dpf. Clarithromycin appears toxic at the highest concentration as evidenced by the development of abnormalities and the increased mortality rate in the drug-exposed embryos compared to the mock control (p=0.028, log-rank test). **(B)** Survival of infected *Mabs* treated at various doses of clarithromycin and compared to untreated infected embryos (≈300 CFU, n=20, representative of three independent experiments). A significant increased survival was observed in the infected-embryos exposed to the highest drug concentration (p=0.029, log-rank test). **(C)** Bacterial loads of untreated or treated-embryos (≈400 CFU). Results are expressed as mean Log_{10} CFU per embryo from three independent experiments. A significant reduction in bacterial burdens with 170X the MIC in drug treated-embryos is observed at 5dpi. **(D)** Spatiotemporal visualization of the infection by *Mabs* expressing dtTomato (≈300 CFU) in untreated or drug treated-embryos. The representative fluorescence and transmission overlay of whole embryos are shown. The yolk is auto-fluorescent. **(E)** Frequency of abscesses in whole untreated or drug treated-embryos over 13dpi (≈300 CFU; average of three independent experiments). Infected embryos developed significantly less abscesses in the presence of clarithromycin at 170X the MIC than untreated infected-embryos. **(F)** Average localization of abscesses of the infected embryos in (E). *Mabs*-infected ZF developed significantly less abscesses within the brain and the spinal when exposed to the highest clarithromycin dose as compared to untreated infected-ZF. For (C) statistics were calculated using one-way ANOVA or for (E) and (F) with Fisher's exact test comparing each category of drug-treated embryos to untreated control. Error bars represent the SEM. **p<0.01.

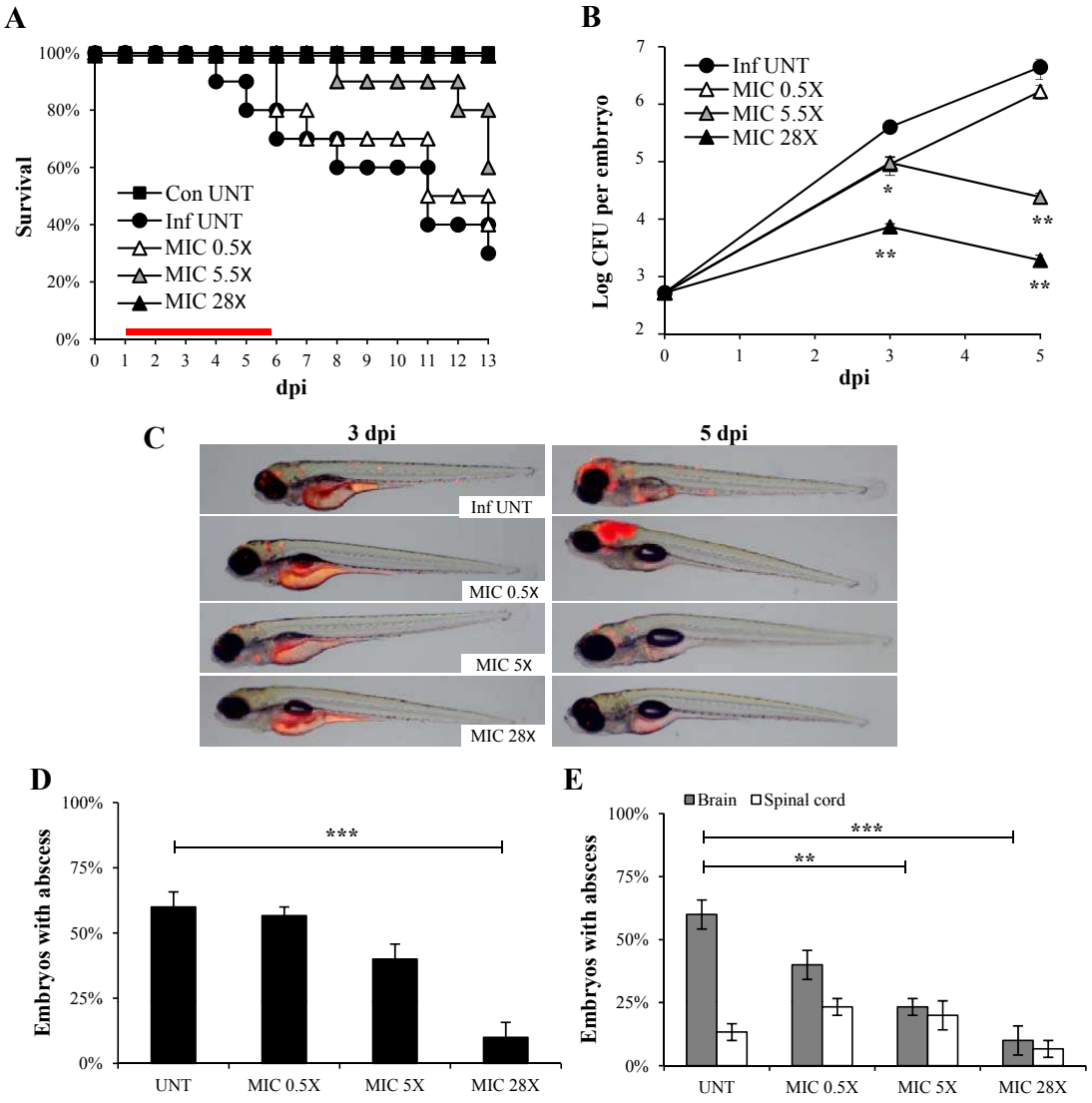

Figure 4. Imipenem treatment cures *M. abscessus*-infected embryos. (A-E) From 1dpi, embryos were exposed for 5 days to imipenem concentrations corresponding to 0.5X, 5X or 28X the MIC. **(A)** Survival of infected R-*Mabs* embryos treated at various doses of imipenem and compared to untreated infected embryos (≈300 CFU, n=20, representative of three independent experiments). Survival of treated R-*Mabs* infected embryos is dose-dependent. Significant increased survival was observed in infected-embryos exposed to 5 X and 28X MIC of imipenem. The red bar indicates the start and duration of treatment. **(B)** Bacterial loads of untreated or imipenem treated-embryos (≈400 CFU). Results are expressed as mean Log_{10} CFU per embryo from three independent experiments. A significant decreased of bacterial load is already observed after 3dpi in the 28X MIC imipenem treated-embryos. **(C)** Spatiotemporal visualization of the infection by R-*Mabs* expressing tdTomato (≈300 CFU) in untreated or imipenem treated-embryos. The representative fluorescence and transmission overlay of whole embryos are shown. **(D)** Frequency of abscesses in whole untreated or imipenem-treated embryos over 13dpi (≈300 CFU, average of three independent experiments). Only the 28X MIC imipenem treated-embryos developed significantly fewer abscesses than untreated infected-embryos. **(E)** Average localization of abscesses of the infected embryos in (D). 5X and 28X MIC of imipenem treated-embryos infected by *Mabs* developed fewer abscesses within the brain than untreated infected-embryos. For (B) statistics were calculated using one-way ANOVA or for (D) and (E) with Fisher's exact test comparing each category of imipenem-treated embryos to untreated control. Error bars represent the SEM. *p=0.02, **p<0.01, ***p<0.001.

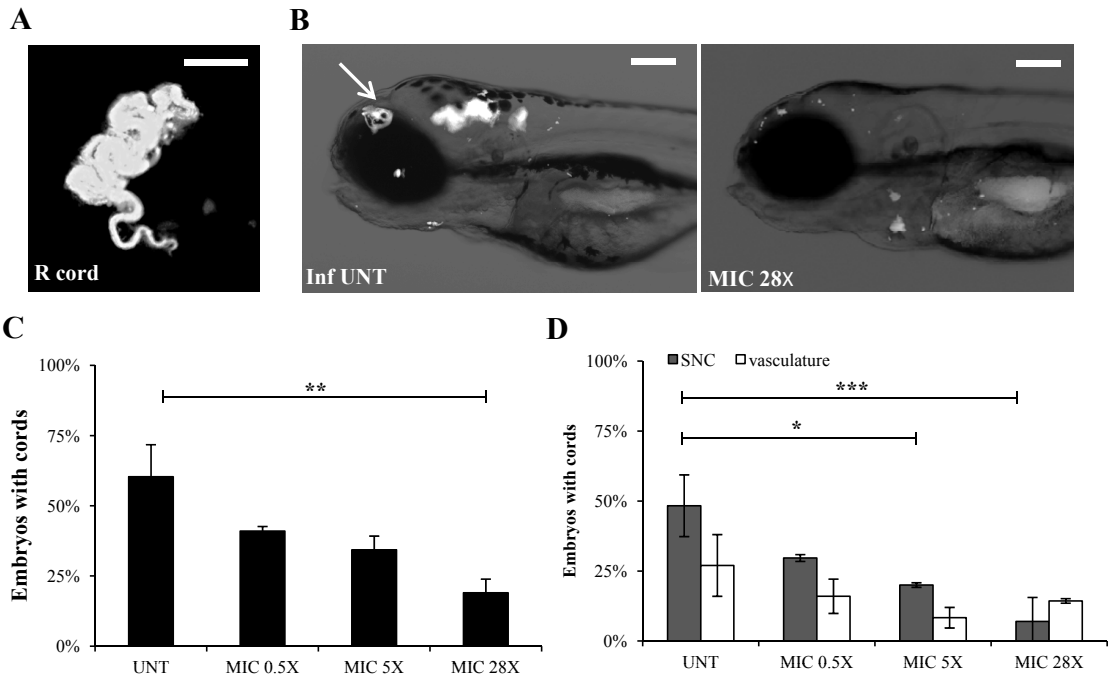

Figure 5. Imipenem treatment decreases the early pathophysiological signs within the CNS. (A-D). tdTomato-expressing R-*Mabs* (≈300 CFU) are injected in 30hpf embryos (n=15, average of three independent experiments). From 1dpi, embryos were exposed to imipenem at 0.5X, 5X or 28X MIC during 5 days. **(A)** Fluorescence microscopy of a typical R serpentine cord. Scale bar, 100µm. **(B)** Fluorescence and DIC overlay of whole heads of a 28X MIC imipenem-treated and untreated infected embryos with fluorescent R-*Mabs* showing serpentine cord (white arrow). Scale bars, 100µm. **(C)** Percentage of embryos with cords in whole untreated and imipenem-treated embryos at 4dpi. A significant reduction in the proportion of embryos with cords was observed when embryos were treated with the highest (28X MIC) imipenem concentration. **(D)** Average localization of cord within the infected embryos in (C). Infected embryos treated with the intermediate (5X MIC) and high (28X MIC) imipenem doses developed significantly fewer serpentine cords within the CNS compared to untreated infected-embryos. For (C) and (D), statistics were calculated using Fisher's exact test comparing each category of imipenem-treated embryos to untreated control. All results are expressed as the average from three independent experiments and error bars represent the SEM.